POLITECNICO DI TORINO
Repository ISTITUZIONALE

Critical issues in the determination of the bentonite cation exchange capacity

Publisher copyright

(Article begins on next page)

29 November 2022

Critical issues in the determination of the bentonite cation exchange capacity for the assessment of the macroscopic density of the solid electric charge

By

Dominijanni A.*, Fratalocchi, E., Guarena N., Manassero M., Mazzieri F.

● **Abstract**

The swelling pressure and transport properties of bentonites are controlled by the electric charge density of solid particles, which is commonly estimated from the laboratory measurement of the cation exchange capacity (CEC). However, the standard ammonium displacement method for CEC determination does not take into account the fabric changes that occur in bentonites under exposure to high salt concentration solutions. A series of laboratory tests was conducted to assess the relevance of such a critical issue, by varying the concentration of the extracting KCl solution with respect to that of the standard test. The obtained results show that the release of the adsorbed ammonium cations depends on the bentonite fabric, which is controlled by the KCl concentration. As a consequence, the ammonium displacement method may provide an unrepresentative estimate of the CEC of bentonites. The methylene blue titration method, despite its apparently more limited accuracy, instead seems to provide a more reliable estimation of the CEC, as the bentonite fabric is maintained dispersed during the test.

List of notations

α empirical coefficient of the fabric boundary surface equation

β empirical coefficient of the fabric boundary surface equation

ρ_{sk} solid-phase density

b_n average half-distance between the platelets in the tactoid

c_0 reference molar concentration in the fabric boundary surface equation

c_s salt molar concentration

$\overline{c}_{sk,0}$ molar concentration per unit solid volume of the solid skeleton electric charge

CEC   cation exchange capacity

d_d d_{Stern}/b_n

d_{Stern} thickness of the Stern Layer around the external surface of the tactoid

e total void ratio

e_m micro-void ratio

f_{Stern} fraction of cations adsorbed in the Stern layer

H height of the bentonite layer in the filtration apparatus of the ammonium displacement method

k hydraulic conductivity of the bentonite layer in the filtration apparatus of the ammonium displacement method

$N_{I,AV}$ average number of lamellae per tactoid

$N_{I,AV0}$ empirical coefficient of the fabric boundary surface equation

2

S total specific surface of bentonite

u_{sw} swelling pressure

1 **Introduction**

2 The transport properties and mechanical behaviour of clay soils with a high specific surface,

3 such as bentonites, are governed by the microscopic interactions that occur between the

4 electrically charged solid particles and the ions that are contained in the pore solution (Lambe,

5 1960; Groenevelt and Bolt, 1969; Sridharan and Rao, 1973; Mitchell, 1991; Moyne and Murad,

6 2002; Mitchell and Soga, 2005; Guimarães et al., 2013; Musso et al., 2017; Revil, 2017a,

7 2017b; Delage, 2019).

8 Bentonites can have either a dispersed fabric, in which clay particles are present as well

9 separated montmorillonite units, or an aggregated structure that consists of packets of particles,

10 or tactoids, within which several clay platelets are in a parallel array. The formation of tactoids is

11 determined by a reduction in the electrical repulsive forces among the clay particles, which is

12 mainly induced by an increase in the salt concentration or a decrease in the solvent dielectric

13 constant of the pore solution.

14 The expected performances of bentonites can be assessed in field applications through

15 physics-based models, which relate the macroscopic constitutive parameters, including

16 hydraulic conductivity, chemico-osmotic efficiency, diffusion coefficient and swelling pressure, to

17 microscopic fabric parameters, such as the average number of montmorillonite lamellae per

18 tactoid, $N_{l,AV}$ (Dominijanni and Manassero, 2012; Shackelford et al., 2019).

19 Manassero (2017) described a physics-based model that was obtained by volume averaging the

20 equations that govern the electric potential distribution, the water flow and the ion transport at

21 the pore scale, and by imposing the condition of macroscopic thermodynamic equilibrium

22 between the pore solution and the external bulk solutions in contact with the bentonite at its

23 boundaries (Dominijanni and Manassero, 2005, 2012; Dominijanni et al., 2006, 2013, 2018).

24 On the basis of such a theoretical approach, the microscopic (pore scale) properties of

25 bentonites are taken into account through a single fundamental parameter, that is the molar

26 concentration per unit solid volume of the solid skeleton electric charge, $\bar{c}_{sk,0}$. This parameter is

27 related to the cation exchange capacity, CEC, as follows (Dominijanni and Manassero, 2012):

28

29 $$\bar{c}_{sk,0} = \frac{1 - f_{Stern}}{N_{l,AV}} \cdot CEC \cdot \rho_{sk} \tag{1}$$

30

31 where ρ_{sk} is the solid-phase density ($\approx$ 2700 kg/m^3) and f_{Stern} is the fraction of cations

32 immobilized in the so-called Stern layer ($\approx$ 0.75$-$0.95).

33 Although CEC determination alone is not sufficient to allow an evaluation of $\bar{c}_{sk,0}$, it plays a

34 fundamental role in relating the physical and chemical properties of bentonite at the pore scale

35 to the macroscopic constitutive parameters. For this reason, a series of experimental tests has

36 been conducted to assess the reliability of the most commonly used CEC measurement

37 methods, including the ammonium displacement method and the methylene blue titration (MB)

38 method.

39

40 **2. Materials and methods**

41

42 *2.1 Bentonite*

43 The powdered bentonite used in this study comes from the same lot and was subjected to the

44 same cyclic-squeezing procedure as in Puma et al. (2015) to remove soluble salts prior to

45 further testing. The main properties of the bentonite are listed in Table 1.

46

47 *2.2 Testing procedures*

48 As far as the ammonium displacement method is concerned, the CEC was determined

49 according to the ASTM D7503-18 procedure, except for the KCl solutions that were used in the

50 final extraction step: in addition to the 1 M KCl solution (standard procedure), extracting

51 solutions with different KCl concentrations (4.5 M, 0.1 M, 0.05 M, 0.025 M, 0.01 M, 0.0025 M,

52 0.001 M) were used together with distilled water (DW) to investigate the effect of changes in the

53 bentonite fabric on the CEC results. The tests were generally performed in duplicate for each

54 extracting solution.

55 The MB test was carried out following the procedure outlined in EUBA (2002). The method is a

56 rapid qualitative procedure that is used in industry for routine quality controls, which provides a

57 measure of the accessible anionic sites in a condition of enhanced dispersion of the clay. This

58 dispersion is obtained by bringing the bentonite suspension to the boil and subsequently titrating

59 the suspension with an anionic dye (methylene blue).

60

61 **3. Test results**

62 The CEC measurement results are listed in Table 2 and plotted in Figure 1. The solid symbols

63 in Figure 1 represent the CEC values obtained from the ammonium release measurements. The

64 values obtained using DW are plotted at 0.0001 M KCl concentration. Considering the average

65 of the measurements for each extracting solution concentration, the maximum value of CEC

66 measured with ammonium was 75.3 meq/100g, which was obtained for the 0.1 M KCl solution

67 (the value of 103 meq/100g for the third replicate at 0.1 M KCl was considered to be an outlier

68 of the dataset and, therefore, neglected). As a result, the maximum CEC value obtained with

69 ammonium was lower than the values obtained with the MB tests (97 and 104 meq/100g; for the

70 sake of simplicity the mean value is plotted in Figure 1). The results suggest that the measured

71 CEC depends on the aggregation state of the bentonite particles. The MB test seems to provide

72 an upper bound of the measured CEC due to the disperse state of the bentonite, which

73 enhances the accessibility of exchange sites with respect to the state of aggregation obtained in

74 the standard test. Despite some scatter in the results, the average CEC versus KCl

75 concentration tends to be practically constant for KCl $>$ 0.1 M, thus suggesting a similar

76 aggregation state of bentonite particles. As the KCl concentration decreased ($<$ 0.1 M), the CEC

77 calculated from the released ammonium also decreased. It should be considered that the

78 amount of K cations available for exchange also decreased. The maximum theoretically

79 measurable CEC, as calculated from the available potassium, is also shown in Figure 1. The

80 measured CEC values for low ($<$ 0.02 M) to practically zero (DW) KCl concentrations are in the

81 13.9 - 23.9 meq/100g range, that is higher than the theoretically predicted values based on the

82 available potassium. A blank test (performed without soil and using a 1 M KCl solution) showed

83 that the ammonium residue in the apparatus at most accounts for 1.3 meq/100g. Therefore, the

84 measured CEC suggests a release of ammonium from the clay that is not related to the

85 adsorption of potassium. According to the test method, washing the clay with isopropanol

86 should remove the excess unbound ammonium acetate; however, the test results suggest that

87 some residual ammonium remains in the clay. A replicate test was performed using 0.0025 M

88   KCl solution and a double wash with isopropanol (240 ml instead of 120 ml), but no significant

89   difference in the measured CEC was observed (Table 2). Therefore, the test results suggest

90   that, even after washing with isopropanol, some unbound ammonium remains entrapped in the

91   bentonite layer. Filtration with low concentration (< 0.02 M KCl) solutions induces a change in

92   bentonite fabric during the test, namely swelling and reorganisation, whereby the release of

93   ammonium is favoured. This is reflected, at the macroscopic scale, by an increase in the

94   average height of the bentonite film that forms in the filtration apparatus, H, at the end of the

95   tests, and a corresponding decrease in the hydraulic conductivity, k. The k value was estimated

96   from the observed flow rate of the filtrate during the addition of the final 50 ml of the extracting

97   solution and from the hydraulic gradient that was established across the bentonite film during

98   filtration. H was equal to 2.5 mm and the average k was estimated to be about 10^{-7} m/s with the

99   1 M KCl solution (standard procedure), whereas H was 8 mm and k was about 10^{-9} m/s with

100   DW.

101

102   **4. Discussion**

103   The observed changes in the hydraulic conductivity of bentonite suggest that the CEC variation,

104   as a function of the extracting KCl solution concentration, can be related to fabric modifications.

105   Manassero et al. (2016, 2018), Dominijanni et al. (2017) and Manassero (2017) modelled

106   bentonite fabric modifications through a fabric boundary surface (FBS), whereby the average

107   number of lamellae per tactoid, $N_{l,AV}$, is related to the salt concentration, c_s, and the micro-void

108   ratio, e_m, which in turn is obtained by subtracting the void space between the platelets of the

109   tactoids from the total void space.

110   A first phenomenological formulation of FBS was proposed by Manassero et al. (2016):

111

112   $$N_{l,AV} = N_{l,AV0} + \frac{\alpha}{e_m} \cdot \left(\frac{c_s}{c_0} + 1 \right) + \beta \cdot e_m \cdot \left[1 - \exp\left(-\frac{c_s}{c_0} \right) \right] \qquad (2)$$

113

114   where c_0 represents the reference molar concentration (= 1 M) and $N_{l,AV0}$, α and β are non-

115   dimensional empirical parameters.

116 The micro-void ratio, e_m, in Eq. 2 can be derived from the total void ratio, e, through the

117 following equation:

118

119 $$e_m = \frac{e \cdot N_{l,AV} - S \cdot \rho_{sk} \cdot b_n \left(N_{l,AV} + d_d - 1 \right)}{N_{l,AV}}$$ (3)

120

121 where b_n is the average half-distance between the platelets in the tactoid ($\approx$ 0.4 nm), S is the

122 total specific surface ($\approx$ 700 m^2/g) and d_d is the thickness of the Stern Layer divided by b_n ($\approx$ 4).

123 Inserting Eq. 3 into Eq. 2 the number of lamellae per tactoid is related to the total void ratio and

124 the salt concentration through a cubic equation, which can be solved analytically or numerically

125 for given values of the parameters $N_{l,AV0}$, α, β, S, ρ_{sk}, b_n and d_d.

126 Although a sufficient number of experimental data is not available for the tested bentonite to

127 determine the FBS parameters, a qualitative analysis was conducted by using the calibration

128 performed by Manassero (2017) on the hydraulic conductivity experimental results obtained by

129 Petrov and Rowe (1997) on a needle-punched geosynthetic clay liner (GCL), which provided

130 $N_{l,AV0}$ = 1.56, α = 8.82, β = 10.01. A plot of the corresponding FBS in the space of the variables

131 $N_{l,AV}$, e_m and c_s is shown in Figure 2. Such an FBS can be regarded as suitable for the analysis

132 of the obtained laboratory data, as the features of the bentonite in the GCL are similar to the

133 ones of the tested bentonite (Table 1) and the GCL hydraulic conductivity is not expected to be

134 influenced by the presence of needle-punched fibres, at least in the range of low salt

135 concentrations (< 0.1 M KCl solution) (Puma et al., 2015).

136 The ability of the proposed FBS to accurately model microstructural changes was verified using

137 a series of experimental results from the literature that included direct measurements of $N_{l,AV}$, on

138 bentonites with similar properties to the ones of the bentonite tested in the present study (Table

139 1). The values of $N_{l,AV}$, which were estimated directly from the ratio of the intra-tactoid to the

140 inter-tactoid pore-space by means of Small Angle X-Ray Scattering Spectroscopy (Muurinen et

141 al., 2013) and Nuclear Magnetic Resonance techniques (Muurinen et al., 2013; Ohkubo et al.,

142 2016), are shown to be in good agreement with the FBS predictions in Figure 3, for a salt

143 concentration c_s = 0.1 M.

144 The total void ratio was estimated, during the washing phase with isopropanol, from the

145 measurement of the bentonite layer thickness to be about 4 and, as a result, $N_{I,AV}$ is calculated

146 through the FBS equation to be about 4.74, assuming $c_s = 0$ as a consequence of the complete

147 removal of the pore aqueous solution.

148 The relation between $N_{I,AV}$ and the KCl concentration, c_s, provided by the FBS for the values of

149 the bentonite void ratio that were estimated at the end of the ammonium displacement tests

150 (Table 2) is shown in Figure 4. The value of the KCl concentration corresponding to $N_{I,AV} = 4.74$

151 is equal to about 0.027 M. As a result, the bentonite is expected to swell during the KCl solution

152 filtration phase and assume a more dispersed fabric when the KCl concentration is lower than

153 0.027 M, while it is expected to flocculate and assume a more aggregated fabric when the KCl

154 concentration is higher than 0.027 M. Such a theoretical threshold value of the KCl

155 concentration is very close to the experimentally found value of 0.02 M, below which the

156 released ammonium overcomes the available potassium.

157 This qualitative result suggests an interpretation of the CEC data that were obtained from the

158 ammonium release measurements. After the washing phase with isopropanol, a portion of

159 mobile ammonium was not removed because of the presence of pores that are less accessible

160 to the advection flux. When the KCl concentration of the extracting solution was lower than

161 about 0.02 M, the dispersion of the bentonite allowed the mobile ammonium ions to be released

162 by opening such pores. Instead, when the KCl concentration of the extracting solution was

163 higher than about 0.02 M, the bentonite flocculated and created additional less accessible pore

164 voids. The potassium cations only had access to a limited portion of the available pores for the

165 highest values of the KCl concentration (≥ 1 M), and, as a result, the exchanged ammonium ion

166 measurements underestimated the effective bentonite CEC.

167

168 **5. Conclusions**

169 The tests performed by varying the KCl solution concentrations showed that the CEC

170 measurements based on ammonium release are influenced by bentonite fabric modifications

171 and may provide an unreliable estimation of the effective density of the exchangeable sites of

172 the bentonite. For this reason, the ammonium displacement method does not seem to be

173   sufficiently accurate to assess the fundamental fabric parameters of coupled hydro-chemo-

174   mechanical models, such as the one proposed by Manassero et al. (2016). The experimental

175   swelling pressure data obtained by Dominijanni et al. (2013) for a saturated sodium bentonite at

176   a void ratio of 4.26 are compared in Figure 5, by way of example, with the theoretical predictions

177   that are obtained by determining $\overline{c}_{sk,0}$ from the measurement of CEC through Eq. 1, with a

178   constant $N_{I,AV}$ value ($N_{I,AV} = 3$) for the investigated range of low salt concentrations (Manassero,

179   2017). The theoretical curve derived from the average CEC provided by the standard

180   ammonium displacement method underestimates the experimental data to a great extent,

181   whereas an acceptable fitting is obtained when the average CEC value provided by the

182   methylene blue titration method is used. As a result, the methylene blue titration method, which

183   is used in industry for routine quality controls, seems to be able to provide a more reliable

184   estimation of CEC, despite its apparently more limited accuracy, as the bentonite fabric is

185   maintained dispersed during the test.

186

References

ASTM D7503-18 Standard Test Method for Measuring the Exchange Complex and Cation Exchange Capacity of Inorganic Fine-Grained Soils.

Delage P (2019) Micro-macro effects in bentonite engineered barriers for radioactive waste disposal. In: Zhan L, Chen Y and Bouazza A (Eds.) Proceedings of the 8th International Congress on Environmental Geotechnics, Hangzhou, China; 28 October - 1 November 2018. Springer, Singapore, pp. 61-80.

Dominijanni A and Manassero M (2005) Modelling osmosis and solute transport through clay membrane barriers. In: Alshawabkleh A, Benson CH, Culligan PJ, Evans JC, Gross BA, Narejo D, Reddy KR, Shackelford CD and Zornberg JG (Eds) Proceedings of the Geo-Frontiers Congress, Austin, Texas (USA), 24-26 January 2005. American Society of Civil Engineers, Reston, Virginia (USA), pp. 349-360.

Dominijanni A and Manassero M (2012) Modelling the swelling and osmotic properties of clay soils. Part II: The physical approach. International Journal of Engineering Science 51: 51-73.

Dominijanni A, Guarena N and Manassero M (2018) Laboratory assessment of semi-permeable properties of a natural sodium bentonite. Canadian Geotechnical Journal 55(11): 1611-1631.

Dominijanni A, Manassero M and Puma S (2013) Coupled chemical-hydraulic-mechanical behaviour of bentonites. Géotechnique 63(3): 191-205.

Dominijanni A, Manassero M and Vanni D (2006) Micro/macro modeling of electrolyte transport through semipermeable bentonite layers. In: Thomas HR (Ed.) Proceedings of the 5th International Congress on Environmental Geotechnics, Cardiff, Wales (UK), 26-30 June 2006. Thomas Telford, London, England (UK), vol. 2, pp. 1123-1130.

Dominijanni A, Manassero M, Boffa G and Puma S (2017) Intrinsic and state parameters governing the efficiency of bentonite barriers for contaminant control. In: Ferrari A and Laloui L (Eds.) Proceedings of the International Workshop on Advances in Laboratory Testing and Modelling of Soils and Shales, Villars-sur-Ollon, Switzerland, 18-20 January 2017. Springer International Publishing AG, Cham, Switzerland, pp. 45-56.

EUBA - European Bentonite Association (2002) Methodology for the determination of the methylene blue value of bentonite.

216 Groenevelt PH and Bolt GH (1969) Non-equilibrium thermodynamics of the soil-water system.

217 Journal of Hydrology 7(4): 358-388.

218 Guimarães LDN, Gens A, Sánchez M and Olivella S (2013) A chemo-mechanical constitutive

219 model accounting for cation exchange in expansive clays. Géotechnique 63(3): 221-234.

220 Lambe TW (1960) A mechanistic picture of shear strength in clay. In Proceedings of the

221 Research Conference on Shear Strength of Cohesive Soil, Boulder, Colorado (USA), June

222 1960. American Society of Civil Engineers, New York (USA), pp. 555–580.

223 Manassero M, Dominijanni A and Guarena N (2018) Modelling hydro-chemo-mechanical

224 behaviour of active clays through the fabric boundary surface. In: Proceedings of China-

225 Europe Conference on Geotechnical Engineering, Vienna, Austria, 13-16 August 2018.

226 Springer, Cham, Switzerland, pp. 1618-1626.

227 Manassero M, Dominijanni A, Fratalocchi E, Mazzieri F, Pasqualini E and Boffa G (2016) About

228 state parameters of the active clays. In: Proceedings of the Special symposium honoring

229 D.E. Daniel, Geo-Chicago 2016, 14-18 August 2016, Chicago, Illinois (USA), pp. 99-110.

230 Manassero M. (2017) On the fabric and state parameters of active clays for contaminant control

231 (2nd ISSMGE Kerry Rowe Lecture). In: Lee W and Lee J-S, Kim H-K and Kim D-S (Eds.)

232 Proceedings of the 19th International Conference of Soil Mechanics and Geotechnical

233 Engineering, Seoul, Korea, 17-22 September 2017, pp. 167-189.

234 Mitchell JK (1991) Conduction phenomena: from theory to geotechnical practice. Géotechnique

235 41(3): 299-340.

236 Mitchell JK and Soga K (2005) Fundamentals of soil behavior (3rd Edition). John Wiley & Sons,

237 New York (USA).

238 Moyne C and Murad MA (2002). Electro-chemo-mechanical couplings in swelling clays derived

239 from a micro/macro-homogenization procedure. International Journal of Solids and

240 Structures 39(25): 6159-6190.

241 Musso G, Cosentini, RM, Dominijanni A., Guarena N and Manassero M (2017) Laboratory

242 characterization of the chemo-hydro-mechanical behaviour of chemically sensitive clays.

243 Rivista Italiana di Geotecnica, vol. 2017 (3): 22-47.

244 Muurinen A, Carlsson T and Root A (2013) Bentonite pore distribution based on SAXS, chloride

245 exclusion and NMR studies. Clay Minerals 48 (2): 251-266.

246 Ohkubo T, Ibaraki M, Tachi Y and Iwadate Y (2016) Pore distribution of water-saturated

247   compacted clay using NMR relaxometry and freezing temperature depression; effects of

248   density and salt concentration. Applied Clay Science 123: 148-155.

249 Petrov RJ and Rowe RK (1997) Geosynthetic clay liner (GCL) - chemical compatibility by

250   hydraulic conductivity testing and factors impacting its performance. Canadian Geotechnical

251   Journal 34: 863-885.

252 Puma S, Dominijanni A, Manassero M and Zaninetta L (2015) The role of physical

253   pretreatments on the hydraulic conductivity of natural sodium bentonites. Geotextiles and

254   Geomembranes 43: 263-271.

255 Revil A (2017a) Transport of water and ions in partially water-saturated porous media. Part 1.

256   Constitutive equations. Advances in Water Resources 103: 119-138.

257 Revil A (2017b) Transport of water and ions in partially water-saturated porous media. Part 2.

258   Filtration effects. Advances in Water Resources 103: 139-152.

259 Shackelford CD, Lu N and Malusis MA (2019) Research challenges involving coupled flows in

260   geotechnical engineering. In: Lu N and Mitchell JK (Eds.) Geotechnical Fundamentals for

261   Addressing New World Challenges. Springer.

262 Sridharan A and Rao VG (1973) Mechanisms controlling volume change of saturated clays and

263   the role of the effective stress concept. Géotechnique 23(3): 359-382.

264

265

Table captions

Table 1. Main properties of the bentonite used in this study and comparison with the data of similar bentonites from the literature (Petrov and Rowe, 1997; Muurinen et al., 2013; Ohkubo et al., 2016) (DW = distilled water).

Table 2. CEC values obtained in the study.

Figure captions

Figure 1. CEC values determined with the ammonium acetate method using different KCl solutions in the final stage of the test and comparison with MB results.

Figure 2. Plot of the fabric boundary surface (FBS) in the three-dimensional space of the variables: average number of lamellae per tactoid, $N_{l,AV}$, micro-void ratio, e_m, and salt molar concentration, c_s.

Figure 3. Comparison between the average number of lamellae per tactoid provided by the Fabric Boundary Surface (continuous line) and the experimental results taken from the literature.

Figure 4. Average number of lamellae per tactoid of the bentonite as a function of the concentration of the extracting KCl solution. The arrows indicate the KCl concentration (c_s = 0.027 M) that corresponds to $N_{l,AV}$ = 4.74, i.e. the average number of lamellae per tactoid after the washing phase with isopropanol (c_s = 0).

Figure 5. Comparison between the swelling pressure of bentonite, as theoretically predicted on the basis of the average CEC value derived from the methylene blue titration method [curve (a) – CEC = (97.4 + 104)/2 = 100.7 meq/100g] and the standard ammonium displacement method [curve (b) – CEC = (73.2 + 60.7)/2 = 66.9 meq/100g], and the experimental data obtained by Dominijanni et al. (2013) (closed circles).

1   Table 1. Main properties of the bentonite used in this study and comparison with the data of
2   similar bentonites from the literature (Petrov and Rowe, 1997; Muurinen et al., 2013; Ohkubo et
3   al., 2016) (DW = distilled water).

Property	This Study	Petrov and Rowe (1997)	Muurinen et al. (2013)	Ohkubo et al. (2016)
Smectite content (%)	> 98	91	84	> 98
Prevalent adsorbed cation	Na^+	Na^+	Na^+	Na^+
Liquid Limit to DW (%)	525	530	-	-
CEC (meq/100g)	97 - 104 [a]	85.8 [b]	80 - 88 [c]	-
Hydraulic conductivity to DW (m/s)	8.0×10^{-12} [d]	1.2×10^{-11} [e]	5.0×10^{-12} [f]	-

4   [a] measured through the methylene blue titration method

5   [b] measured through the Ag-Thiourea exchange for Na^+ and K^+, the KCl exchange for Mg^{2+} and

6   Ca^{2+}

7   [c] measured through the Cu(II)-Triethylentetramine exchange method

8   [d] measured at a 27.5 kPa confining effective stress

9   [e] measured at a 35 kPa confining effective stress

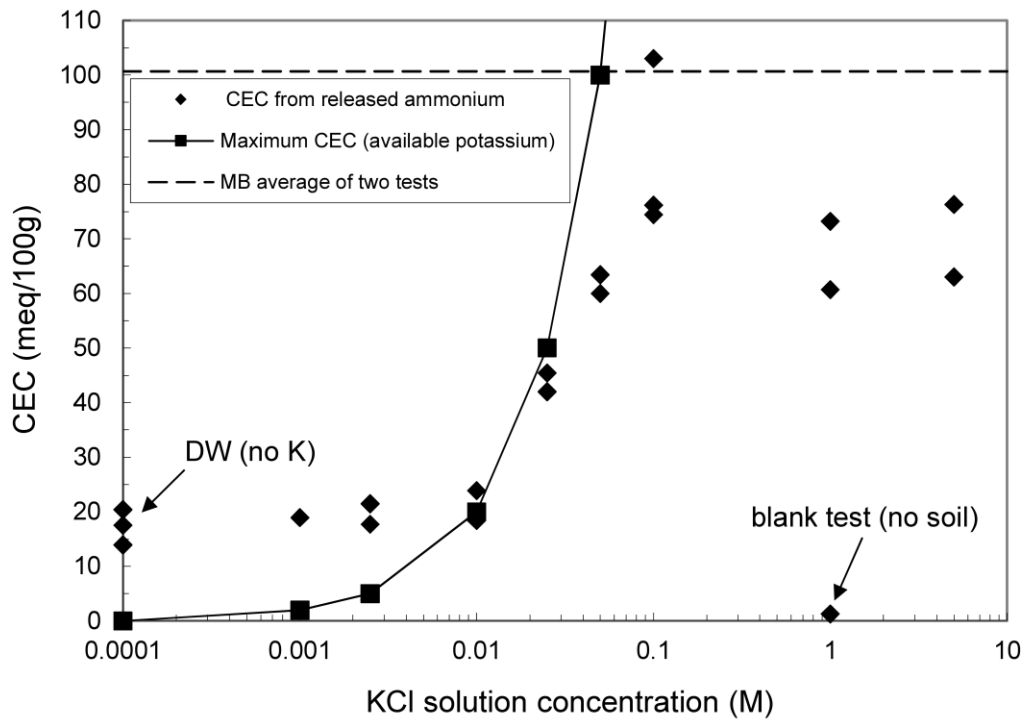10   [f] measured at a bulk dry density equal to 517 kg/m^3

11

12

13   Table 2. CEC values obtained in this study.

		Test 1 (meq/100 g)	Test 2 (meq/100 g)	Test 3 (meq/100 g)	Note
ASTM D7035 (standard and modified procedure)	Estimated bentonite void ratio, e [*]				
DW	14	17.5	20.4	13.9	
0.001 M	12	18.9	-	-	
0.0025 M	12	21.4	17.7	-	
0.0025 M	12	21.5	-	-	Double wash with isopropanol
0.01 M	10	23.9	18.4	-	
0.025 M	8	42.0	45.4	-	
0.05 M	7	60.0	63.4	-	
0.1 M	6	76.2	74.4	103	
1 M (standard)	4	73.2	60.7	-	
1 M (standard)	-	1.3	-	-	Blank test (no soil)
4.5 M	3	63.0	76.3	-	
Methylene Blue (EUBA)					
	-	97.4	104	-	

14   [*] total void ratio estimated from the detection of the bentonite layer thickness within the filtration

15   apparatus at the end of the ammonium displacement tests

16

17

Figure 1. CEC values determined with the ammonium acetate method using different KCl solutions in the final stage of the test and comparison with MB results.
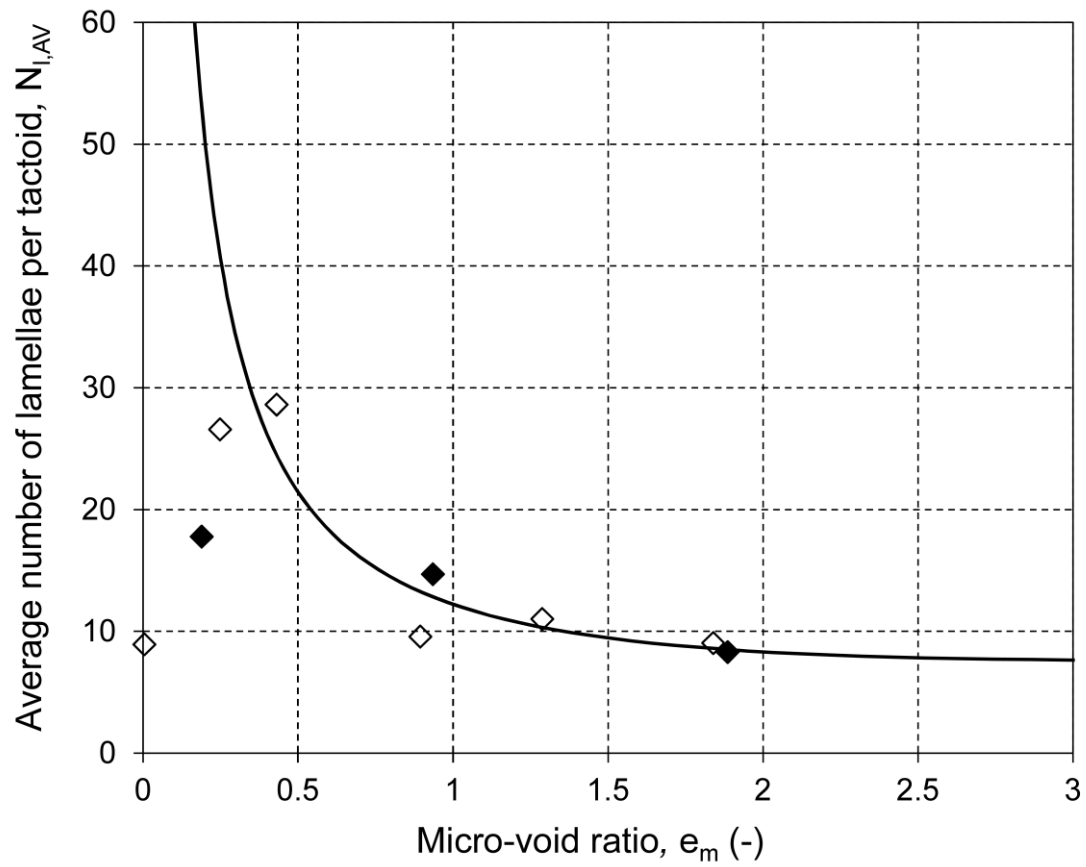
Figure 2. Plot of the fabric boundary surface (FBS) in the three-dimensional space of the variables: average number of lamellae per tactoid, $N_{l,AV}$, micro-void ratio, e_m, and salt molar concentration, c_s.
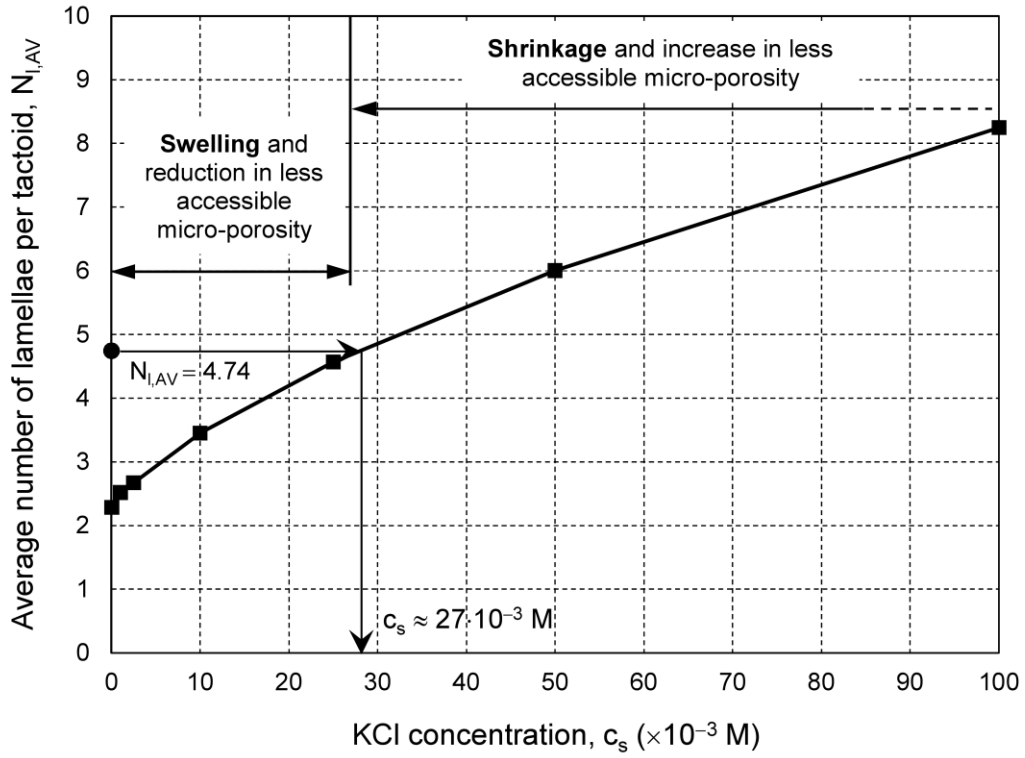
Figure 3. Comparison between the average number of lamellae per tactoid provided by the Fabric Boundary Surface (continuous line) and the experimental results taken from the literature.

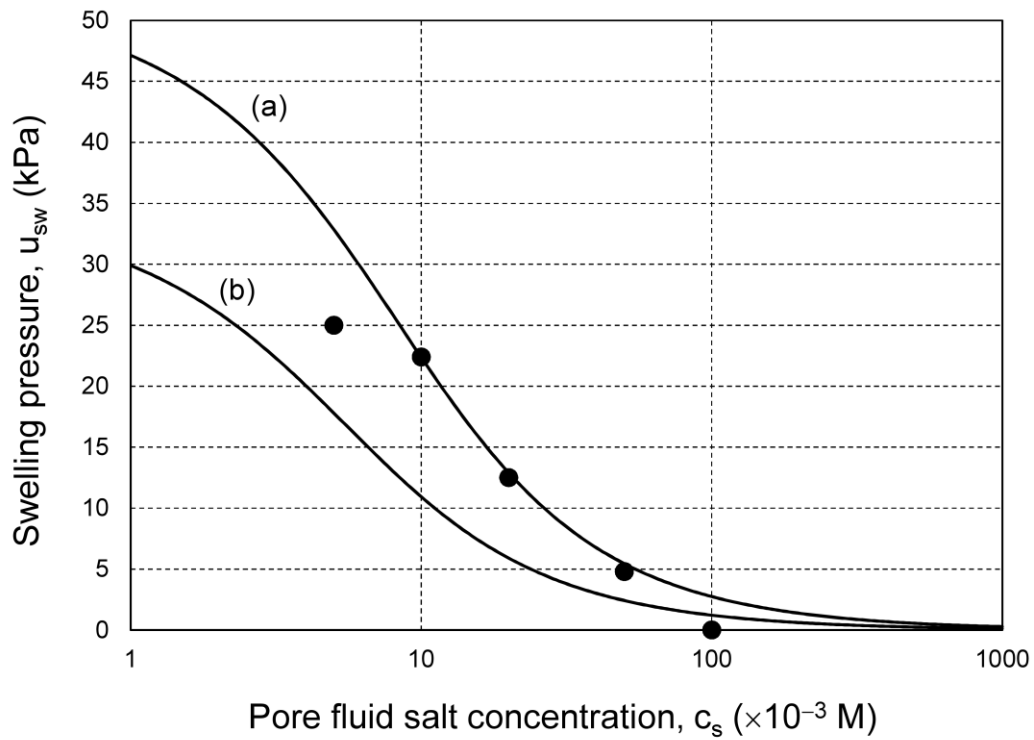Figure 4. Average number of lamellae per tactoid of the bentonite as a function of the concentration of the extracting KCl solution. The arrows indicate the KCl concentration (c_s = 0.027 M) that corresponds to $N_{I,AV}$ = 4.74, i.e. the average number of lamellae per tactoid after the washing phase with isopropanol (c_s = 0).

Figure 5. Comparison between the swelling pressure of bentonite, as theoretically predicted on the basis of the average CEC value derived from the methylene blue titration method [curve (a) – CEC = (97.4 + 104)/2 = 100.7 meq/100 g] and the standard ammonium displacement method [curve (b) – CEC = (73.2 + 60.7)/2 = 66.9 meq/100 g], and the experimental data obtained by Dominijanni et al. (2013) (closed circles).